Journal of Marine Systems 126 (2013) 82–93

Contents lists available at ScienceDirect

Journal of Marine Systems

journal homepage: www.elsevier.com/locate/jmarsys

The geochemical behavior of natural radionuclides in coastal waters: A modeling study for the Huelva estuary

Raúl Periáñez [a,*], Almudena Hierro [b], Juan Pedro Bolívar [b], Federico Vaca [b]

[a] Dpt Física Aplicada I, ETSIA, Universidad de Sevilla, Ctra Utrera km 1, 41013-Sevilla, Spain
[b] Dpt Física Aplicada, EPS La Rábida, Universidad de Huelva, Ctra Palos s/n, 21819-Huelva, Spain

ARTICLE INFO

Article history:
Received 6 September 2011
Received in revised form 21 May 2012
Accepted 2 August 2012
Available online 14 August 2012

Keywords:
Numerical modeling
Dispersion
Natural radionuclides
Odiel–Tinto estuary
Acid mine drainage
Phosphogypsum

ABSTRACT

A numerical model to study the behavior and distribution of natural radionuclides in sediments of an estuary (Odiel and Tinto rivers, SW Spain) affected by acid mine drainage and industrial activities has been developed. The model solves water circulation due to tides and river stream flows. The dispersion model includes uptake/release reactions of radionuclides between the dissolved phase and bed sediments in a dynamic way, using kinetic transfer coefficients. Seasonal pH and chlorinity distributions are simulated, and a formulation has been developed to consider these seasonal variations on kinetic coefficients. Calculated concentrations of ^{226}Ra and ^{238}U in sediments have been compared with measurements from four seasonal sampling campaigns. Numerical experiments have been carried out to study the relative significance of the different radionuclides sources into the estuary as well as the effect of the two components of water circulation (tides are river flows) on radionuclide dispersion patterns.

1. Introduction

Acid mine drainage (AMD) is caused by the weathering of sulfide rich mining materials, and may persist for centuries after closing the mine. AMD is polluted water which normally contains high levels of sulfates, metals and metalloids and is characterized by a low pH (de la Torre et al., 2011).

The Odiel–Tinto rivers, in the southern Iberian Peninsula, are affected by AMD since they drain the Iberian Pyrite Belt (Sainz and Ruiz, 2006), one of the most important mining areas in the south of Europe. Mineral resources have been extracted in the last 5000 years during two main periods: the Roman age and the last two centuries. During the last period, intensive exploitation has led to a relevant environmental impact caused by AMD. Both rivers form a fully mixed tidal estuary which surrounds the town of Huelva. Rivers join at the south of this town and then flow together to the Atlantic Ocean (see Fig. 1).

Additionally, a fertilizer processing complex is located near Huelva town, by the Odiel River estuary. These factories generate a by-product called phosphogypsum, which contains enhanced levels of natural radionuclides and heavy metals (Rajkovic et al., 1999; Van der Heijde et al., 1988). Phosphogypsum has been stored in open air piles located in the salt marsh of the Tinto River until the end of 2010. These piles cover 1600 ha, of which 600 ha have been restored. There is a total amount of 80 Mt of stored phosphogypsum. Water leached from the phosphogypsum piles into the Tinto River contains significant levels of the pollutants mentioned above (Bolívar et al., 2009); in particular, some 50–100 Bq/l of ^{238}U and some 1–5 Bq/l of ^{226}Ra.

Several works have been published in the recent past concerning the contamination of the Odiel-Tinto estuary by metals (de la Torre et al., 2011; Martín et al., 2002; Respaldiza et al., 1993) and radionuclides (Absi et al., 2004; Bolívar et al., 2000, 2002; Martínez-Aguirre et al., 1996). Indeed, the Odiel–Tinto estuary constitutes one the most metal and radionuclide polluted estuaries in the world (Ruiz, 2001).

Even more recently (Hierro, 2009; Hierro et al., 2012), the presence of natural radionuclides in sediments of the Odiel and Tinto rivers and estuary has been investigated in detail. Four sampling campaigns (one per season) have been carried out to study the behavior of different natural radionuclides under the variable pH and salinity conditions which occur in the estuary. Interpretation of results is not an easy task due to the many factors in play; the mains are tidal mixing, pH and salinity gradients and uptake/release reactions of radionuclides between water and sediments. The solid phase may act as a sink or as a source of radionuclides to the water column, depending on the concentration of radionuclides in each phase and on the rates governing the adsorption and release reactions, which also depend on environmental conditions (pH, temperature, and salinity).

Thus, the objective of this work consists of developing a numerical model of the estuary, including all processes mentioned above. It solves the hydrodynamics of the estuary and the dispersion of natural radionuclides, including the interactions between the dissolved and solid (bottom sediments) phases. An earlier and simplified modelling

* Corresponding author.
E-mail address: rperianez@us.es (R. Periáñez).

0924-7963/$ – see front matter © 2012 Elsevier B.V. All rights reserved.
http://dx.doi.org/10.1016/j.jmarsys.2012.08.001

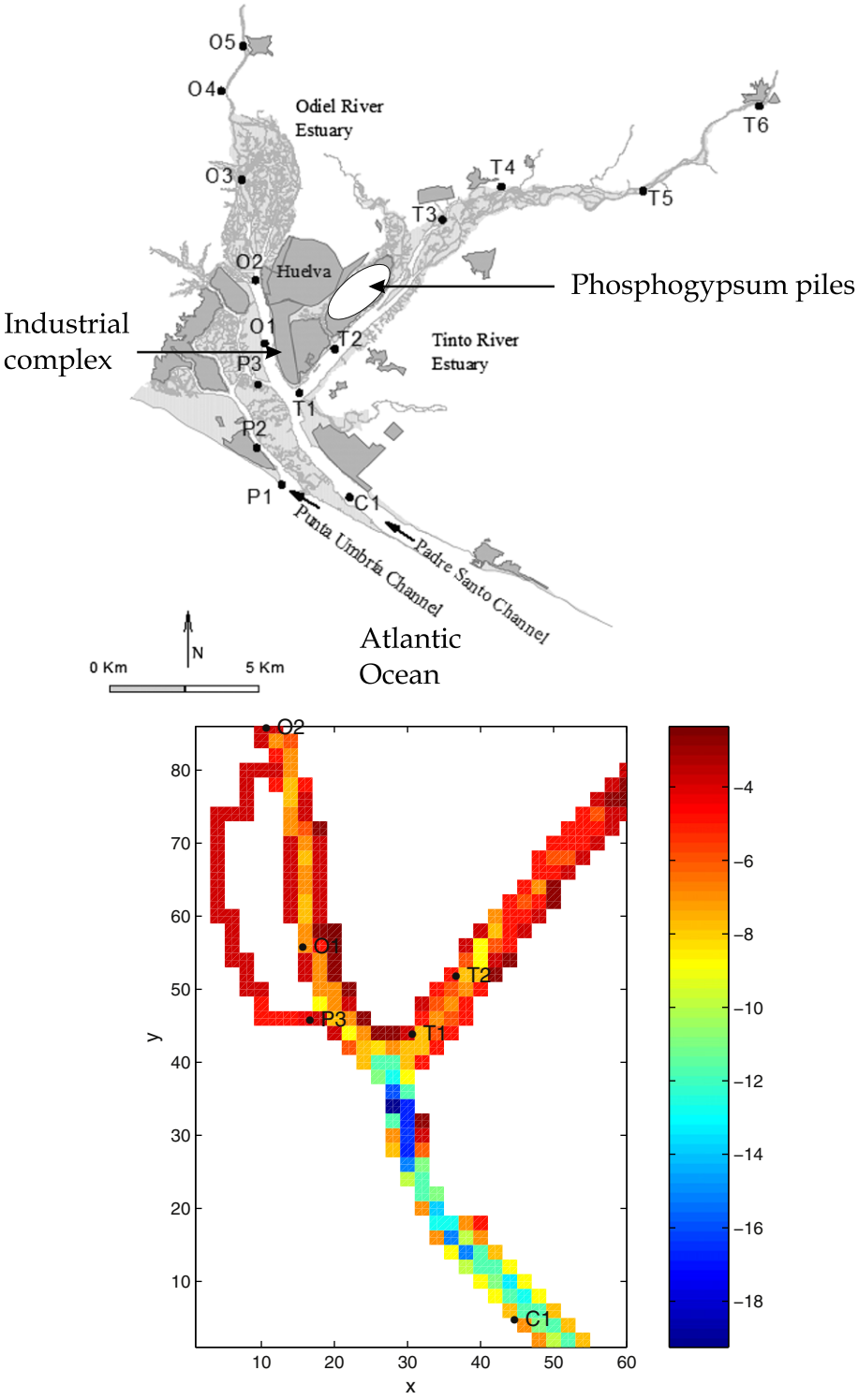

Fig. 1. Map of the estuary (up) and model domain (down) with location of sampling points. The colorbar gives water depths in m. Each number in the *x* and *y* axis gives the grid cell number (thus each unit corresponds to 125 m).

study of the estuary has already been carried out by the authors (Periáñez et al., 2005). This model was developed and applied to the study of the redissolution of ^{226}Ra from previously contaminated estuarine sediments.

Essentially, the model solves the water circulation in the estuary, caused by tidal motions and river stream flows. This circulation is used to calculate seasonal pH and chlorinity distributions. Uptake/release reactions for radionuclides between water and sediments are described in a dynamic way, using kinetic transfer coefficients. In particular, a two-step model consisting of two consecutive reversible reactions has been applied. A new formulation has been developed to consider how pH and chlorinity variations affect kinetic rates. Calculated currents, pH and chlorinity distributions are then used to simulate the dispersion of radionuclides. The model has been applied to ^{226}Ra and ^{238}U. Calculated radionuclide concentrations in sediments have been compared with measurements for the four seasonal sampling

campaigns described in Hierro (2009) and Hierro et al. (2012). Some numerical experiments have been carried out to investigate the relative significance of the different radionuclide supplies to the estuary. Also, the effect of tidal currents and currents due to river flows on the dispersion patterns of radionuclides has been studied by means of numerical experiments.

The model is detailed described in the next section. Later, results are presented and discussed.

2. Model description

The system under study is divided into a number of grid cells or compartments. Two phases are present in each grid cell: dissolved and active bottom sediments (particles with a diameter of <62.5 μm). Thus, the active sediments correspond to muddy sediments, following the Wentworth scale of sediment grain size (see for instance Pugh, 1987). Larger grain sizes are not considered since it has been found (Aston et al., 1985) that virtually all the radioactivity is associated with the muddy sediment. This result has also been obtained with a model in which a large grain size sediment fraction is included (Periáñez, 1999). Suspended matter particles have not been considered in the model, and thus deposition processes and erosion of the sediment have been neglected. This approximation is used since the radionuclide adsorption capacity of suspended matter, given the typical suspended matter concentrations in the estuary, is very small compared with that of the sediment (this is fully justified in Section 3.2.1). Moreover, the erosion-deposition rates, obtained from a suspended matter model of the estuary (Periáñez et al., 1996), are small (of the order of 10^{-2} g/cm^2 year). Thus, as an approximation, it has been considered that the most important phases controlling radionuclide transport are the dissolved phase and the bottom sediment. This approximation seems realistic given the generally good agreement between model results and observations (see below).

The water circulation is obtained solving the 2D shallow water hydrodynamic equations. Instead of solving these equations simultaneously with the dispersion equations, the hydrodynamic model is calibrated and validated in advance to speed up simulations. Once the hydrodynamics have been validated, standard tidal analysis (Pugh, 1987) is used to determine tidal constants (amplitude and phase) for each grid cell. These constants are evaluated for both components of the flow and for the water elevation, and for all the tidal constituents included in the model (M_2 and S_2). Once tidal constants are known, computation of flow and water elevation just involves the calculation and addition of a few cosine terms, since the constants are stored in files that are read by the dispersion model. The net residual flow due to river discharges over the estuary must also be calculated by the hydrodynamic model and added to the instantaneous flow obtained from the tidal constants.

Water circulation is then used to calculate pH and chlorinity distributions over the estuary. Seasonal distributions have been calculated. These are required since adsorption/release processes of radionuclides between the dissolved phase and the sediment are affected by pH and Cl^- concentrations.

Finally, instantaneous tidal currents, seasonal residual currents and seasonal pH and chlorinity distributions are used to simulate radionuclide dispersion. A sequence of consecutive calculations is thus required:

1. Run the hydrodynamic model with tidal forcing, separately for each constituent, until stable oscillations are obtained. Then tidal constants are calculated and stored.
2. Run the hydrodynamic model using seasonal river flows (one run per season) until a steady circulation is obtained. Each seasonal current field is stored.
3. Run the transport model to calculate pH and chlorinity distributions over the estuary. One run per season is carried out. Seasonal fields are stored.
4. Run the transport model for each radionuclide, with geochemical reactions, for the whole simulation period (2003–2009). Linear interpolation is used between the four seasonal values of river flow currents, pH and chlorinity. Instantaneous tidal currents and water surface elevations are used.

A summary of model equations is given in what follows.

2.1. Water circulation

The 2D, depth-averaged, barotropic shallow water hydrodynamic equations are (see for instance Kowalick and Murty, 1993; Periáñez, 2005):

$$\frac{\partial z}{\partial t}+\frac{\partial}{\partial x}[(D+z)u]+\frac{\partial}{\partial y}[(D+z)v]=0 \tag{1}$$

$$\frac{\partial u}{\partial t}+u\frac{\partial u}{\partial x}+v\frac{\partial u}{\partial y}+g\frac{\partial z}{\partial x}-\Omega v+k\frac{u\sqrt{u^2+v^2}}{D+z}=0 \tag{2}$$

$$\frac{\partial v}{\partial t}+u\frac{\partial v}{\partial x}+v\frac{\partial v}{\partial y}+g\frac{\partial z}{\partial y}+\Omega u+k\frac{v\sqrt{u^2+v^2}}{D+z}=0 \tag{3}$$

where u and v are the depth averaged water velocities along the x and y axis, D is the depth of water below the mean sea level, z is the displacement of the water surface above the mean sea level measured upwards, Ω is the Coriolis parameter ($\Omega=2w\sin\lambda$, where w is the earth's rotational angular velocity and λ is latitude), g is acceleration due to gravity and k is the bed friction coefficient.

The first equation represents mass conservation and the other two momentum conservation. As a typical Atlantic tidal estuary, this is a fully mixed one (Ibañez et al., 2009). Thus, the use of a 2D model is justified since the estuary is very shallow (maximum depth around 19 m) and well mixed in the vertical. Moreover, it is widely known that it is safe to neglect density differences in tidal computations (Dyke, 2001). Since the estuary is relatively narrow (generally less than 1 km), only winds blowing during enough time in the direction of the channel would have a significant effect on currents and, then, on sediment dynamics. Moreover, wind wave action inside the estuary is weak. Consequently, as a first approximation, winds have been neglected in the calculations.

2.2. pH and chlorinity

The dispersion of H^+ and Cl^- ions is simulated to obtain pH and chlorinity distributions respectively. These are conservative tracers, remaining in solution, in the area of interest. Thus, their transport is governed by an advection/diffusion equation in a 2D form for depth-averaged flow:

$$\frac{\partial(Hb)}{\partial t}+\frac{\partial(uHb)}{\partial x}+\frac{\partial(vHb)}{\partial y}=\frac{\partial}{\partial x}\left(HK_D\frac{\partial b}{\partial x}\right)+\frac{\partial}{\partial y}\left(HK_D\frac{\partial b}{\partial y}\right) \tag{4}$$

where total depth is $H=D+z$, K_D is the diffusion coefficient and b is the concentration of H^+ or Cl^- ions for pH and chlorinity simulations respectively.

2.3. Geochemical processes

Adsorption and desorption reactions are described in terms of kinetic transfer coefficients. Thus, the adsorption process (transfer of radionuclides from water to the sediment) will be governed by a coefficient k_1 and the inverse process (desorption to the dissolved phase) by a coefficient k_2. However, some experiments have shown (Ciffroy et al., 2001; El Mrabet et al., 2001) that a two-step kinetic model consisting of two consecutive reactions is more appropriate

than a one-step model, consisting of a single reversible reaction, to simulate both the sorption and release kinetics. This 2-step model has already been tested in other environments, and has been shown to describe the process of redissolution of radionuclides from contaminated marine sediments (Periáñez, 2003, 2004a). The exchange model considers two successive reversible reactions. The first describes a reversible isotopic or ion exchange process between dissolved radionuclides and some non-specific sites present on particle surfaces. The second slower reaction represents a reversible sorption to more specific sites. They can be represented as follows:

$$R + XS_1 \rightleftharpoons_{k_2}^{k_1} RS_1 + X \tag{5}$$

$$S_2 + RS_1 \rightleftharpoons_{k_4}^{k_3} RS_2 + S_1 \tag{6}$$

where k_3 and k_4 are the kinetic transfer coefficients, or sorption and release velocities respectively, for the second reaction, R is the dissolved radionuclide, X is a competitive element that can be replaced by R on sites S_1 and RS_i is the radionuclide bound to sites S_i of the solid particle.

The adsorption process is a surface phenomenon that depends on the surface of particles per water volume unit into the grid cell. This quantity has been denoted as the exchange surface (Periáñez, 2003, 2004a, 2008, 2009). Thus:

$$k_1 = \chi_1 S_E \tag{7}$$

where S_E is the exchange surface and χ_1 is a parameter with the dimensions of a velocity. It is denoted as the exchange velocity (Periáñez, 2003, 2004a, 2008, 2009).

As a first approach, assuming spherical sediment particles and a step function for the grain size distribution of particles, it can be shown (see references above) that

$$S_E = \frac{3Lf(1-p)\phi}{\bar{r}H} \tag{8}$$

where $\bar{r}$ is the mean radius of sediment particles, H is the total water depth, L is the average mixing depth (the distance to which the dissolved phase penetrates the sediment), f gives the fraction of active sediment, p is sediment porosity and ϕ is a correction factor that takes into account that not all the exchange surface of the sediment particle is in contact with water since part of it can be hidden by other particles. It is implicitly assumed that the radionuclide concentration in pore waters of the sediment, in a sediment layer of thickness L inside which the sediment is homogeneous, corresponds to the concentration in the water column. On the other hand, diffusion of radionuclides to deeper sediment layers has been neglected due to the low sedimentation rates in the area (Periáñez et al., 1996). This formulation has been successfully used in all modeling works cited above. Real particles are not spheres, but with this approach it is possible to obtain an analytical expression for the exchange surface (Duursma and Carroll, 1996).

As described before (Nyffeler et al., 1984; Periáñez, 2009) k_1 (thus χ_1) is the essential parameter describing the tracer geochemical behavior. Moreover, some experiments in Huelva estuary (Laissaoui et al., 1998) have shown that only k_1 varies significantly with electrical conductivity, k_2 remaining constant. Thus, the transfer coefficient k_2 is considered constant. It is assumed that the second reaction is not affected by water environmental conditions, since it occurs once radionuclides have already been fixed to the solid particle. Thus, k_3 and k_4 are considered constants as well.

The formulation given in Laissaoui et al. (1998) for the dependence of the exchange velocity upon chlorinity, S, which is deduced from the theory of Abril and Fraga (1996), is used:

$$\chi_1 = \chi_1^0(1-\delta) \tag{9}$$

where

$$\delta = \frac{S}{S+S_0} \tag{10}$$

In these equations χ_1^0 is the freshwater value of the exchange velocity and S_0 is the chlorinity value at which 50% of saturation occurs (Laissaoui et al., 1998). It must be noted that as chlorinity increases, the transfer of radionuclides to the solid phase decreases due to competition effects of radionuclides with ions dissolved in water. The relations given above have been tested through laboratory experiments (Laissaoui et al., 1998). Indeed, the best agreement with experiments is obtained with $S_0 = 15.8$, which has been used in the model.

It is also required to describe the dependence of the exchange velocity with pH. Since k_1 and the sediment-water distribution coefficient, k_d, are proportionally related, we base on the fact that the k_d increases with increasing pH (USEPA, 1999), which has also been deduced by Abril and Fraga (1996). A mathematical function $g(pH)$, ranging between 0 and 1, which modulates the observed behavior of k_d with pH (USEPA, 1999) has been constructed. It has the form:

$$g(pH) = \frac{1}{\exp[-\alpha(pH-\beta)]+1} \tag{11}$$

where β is the pH at which some 50% of precipitation occurs and α controls how abrupt is the k_d increase with pH increase. These parameters have been fitted to reproduce the observations in USEPA (1999) and it has been found $\alpha = \beta = 5$.

Thus, the final dependence of the exchange velocity with chlorinity and pH (note that the k_d is proportional to rate k_1 as mentioned above) is written as follows:

$$\chi_1 = \chi_1^0 F(S,pH) = \chi_1^0 \left(\frac{S}{S+S_0}\right) \max[g_{min}, g(pH)] \tag{12}$$

$g_{min} = 0.001$ is just a threshold value to avoid $\chi_1 \simeq 0$ at low pH. A graphical representation of the function F, modulating the freshwater exchange velocity, may be seen in Fig. 2.

2.4. Radionuclide dispersion

The equation that gives the temporal evolution of activity concentration in the dissolved phase, C_d (Bq/m^3), is:

$$\frac{\partial(HC_d)}{\partial t} + \frac{\partial(uHC_d)}{\partial x} + \frac{\partial(vHC_d)}{\partial y} = \frac{\partial}{\partial x}\left(HK_D \frac{\partial C_d}{\partial x}\right) + \frac{\partial}{\partial y}\left(HK_D \frac{\partial C_d}{\partial y}\right) - k_1 C_d H + k_2 A_s L \rho_s f \phi \tag{13}$$

where A_s (Bq/kg) is activity concentration in the non specific sites of the active sediment and ρ_s is the sediment bulk density expressed in kg/m^3. The kinetic coefficient k_1 is given by Eqs. (7), (8) and (12). An external source of radionuclides should be added to this equation at the points where it exists.

The equation for the temporal evolution of activity concentration in the non-specific sites of the active sediment fraction (Bq/kg) is:

$$\frac{\partial A_s}{\partial t} = k_1 \frac{C_d H}{L\rho_s f} - k_2 A_s \phi - k_3 A_s + k_4 \ A_s^* \tag{14}$$

where A_s^* is activity concentration in the specific sites of the active sediment. The equation for the specific sites is:

$$\frac{\partial A_s^*}{\partial t} = k_3 A_s - k_4 \ A_s^*. \tag{15}$$

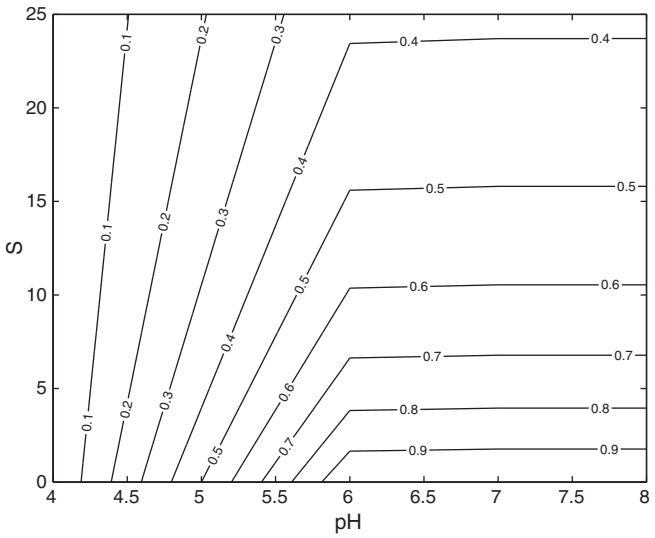

Fig. 2. Function $F(S, pH)$, modulating the freshwater exchange velocity.

The total concentration of radionuclides in the sediment, A_{tot}, is computed from:

$$A_{tot} = f\left(A_s + A_s^*\right). \tag{16}$$

2.5. Computational scheme

The hydrodynamic equations are solved using an explicit finite difference scheme (see for instance Periáñez, 2005). The grid cell size is $\Delta x = \Delta y = 125$ m. Water depths were introduced for each grid cell from bathymetric maps. The computational domain may be seen in Fig. 1. Time step is fixed as $\Delta t = 6$ s to solve hydrodynamics. The CFL criterion (see for instance Kowalick and Murty, 1993) is satisfied with these selections. In order to simulate tides, water elevations are specified for each time step along the southern boundary from observations. A radiation condition (Periáñez, 2005) is applied along the northern and eastern open boundaries. Currents produced by the mean seasonal river flows are simulated specifying such river flows at the northern (Odiel) and eastern (Tinto) open boundaries of the domain, until a steady situation is achieved. Non-linear interactions between tidal constituents and between tides and mean flows are removed if a simple addition of hydrodynamic model results is carried out. However, this is a common practice in transport modeling (Elliott and Clarke, 1998; Periáñez, 2009; Proctor et al., 1994).

Computed tides and seasonal currents are then used to obtain mean seasonal pH and chlorinity distributions. Boundary conditions now consist of specifying H^+ or Cl^- ion concentrations along open boundaries. These concentrations have been measured in the four sampling campaigns, one per season, which have been carried out in the estuary (Hierro, 2009; Hierro et al., 2012). Computed distributions for each season are stored in files. These files are then read by the code which calculates radionuclide dispersion to evaluate the function F (Eq. (12)) for each grid cell and time step. Linear interpolation is used between the four seasonal values of river flow currents, pH and chlorinity.

The MSOU (Monotonic Second Order Upstream) explicit scheme is used to solve the advective transport in the dispersion equation of dissolved radionuclides, pH and S (Vested et al., 1996). A second order accuracy scheme has also been used to solve the diffusion terms (Kowalick and Murty, 1993). Time step in the dispersion model is 30 s, since stability conditions are less restrictive than the CFL criterion. Mass conservation and consistency of the numerical procedure have been carefully checked.

The simulation period extends from 2003 to September 2009, when the last sampling campaign was carried out. Note that almost 7 years have been simulated using a rather small time step and that tidal currents are explicitly included in the simulations. Computation times are reasonably small (about two hours on a PC) thanks to the tidal analysis techniques which have been applied. Boundary conditions in the radionuclide dispersion model consist of specifying radionuclide concentrations from the measurements in Hierro et al. (2012) and Hierro (2009) along open boundaries of the computational domain. Seasonal values were specified for each radionuclide. Linear interpolation between seasons is used to obtain time-varying boundary conditions along the simulation time. Radionuclide concentrations in sediments are obtained from the model in the same dates when sediment samples were collected.

An earlier version of this model (Periáñez et al., 2005) was applied to simulate the self-cleaning of the estuary when direct discharges from the fertilizer complex ceased in 1998. Simulations covered 4 years, until the end of 2002. Results showed reasonable agreement with measurements. Now, radionuclide concentrations in water and sediments provided by such simulations are used as initial conditions for the new simulations, with the new model version, starting in 2003.

3. Results and discussion

3.1. Currents, pH and chlorinity

The hydrodynamic model has been calibrated and tested in a previous work (Periáñez et al., 2005), thus results are not repeated here. The calibration consisted of selecting the optimum value for the bed friction coefficient. Computed current magnitudes and directions were compared with observations. Both set of data were in good agreement (see the indicated reference).

Since tidal mixing is explicitly calculated, the diffusion coefficients must be chosen with respect to the real dispersion coefficient and to that of the subgrid, required to diffuse patches which become too small to be described correctly by the grid size and the numerical scheme. Lam et al. (1984) gave an empirical relationship linking a given patch size to a dispersion coefficient:

$$K_D = 5 \times 10^{-4} d^{1.2} \tag{17}$$

where d is the diameter of the patch. Considering that three grid cells are an acceptable lower limit for the smaller patches to be described by the model (Breton and Salomon, 1995), the present grid size corresponds to a dispersion coefficient $K_D = 0.61$ m^2/s, which is constant over the estuary. This way of defining the diffusion coefficient has been successfully used in previous modeling studies in Huelva estuary (Periáñez, 2002; Periáñez et al., 2005) and other areas (Periáñez, 2008, 2009).

A comparison between calculated and measured pH and chlorinity values (Hierro, 2009; Hierro et al., 2012) along the estuary for the four seasonal sampling campaigns may be seen in Figs. 3 and 4 respectively. The seasonal variations of these magnitudes, as well as their spatial variations along the estuary, are generally well described by the model. It may be seen that pH is very uniform along the Odiel River. There is a significant acidification of Tinto River waters during spring and winter, when river flow is higher, since upstream water, heavily affected by AMD, is transported downstream to the estuary. A similar behavior is observed for chlorinity. Highest values are obtained during summer, due to the low river flows. As an additional example, a map showing the pH distribution over the estuary during spring may be seen in Fig. 5.

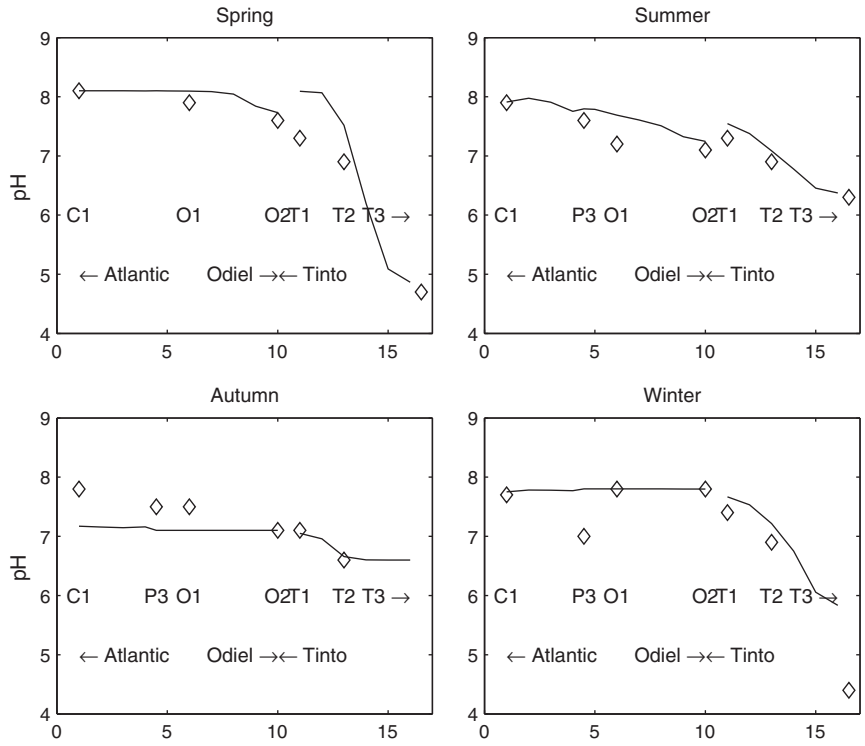

Fig. 3. Comparison between measured (points) and calculated (lines) pH values along the estuary for each sampling campaign. The Odiel River extends in the *x* axis from 1 to 10 and the Tinto River from 10 (confluence with Odiel) to 15. The name of each sample is indicated, and point positions may be seen in the map in Fig. 1.

3.2. Radionuclide dispersion

3.2.1. Parameters

The mean radius of active sediment particles is taken as $R = 15$ μm and the average bulk density of sediments has been measured: $\rho_s = 900$ kg/m^3. Sediment porosity has been deduced from this value and the typical particle density ($\rho = 2600$ kg/m^3) through the known relation $\rho_s = \rho(1-p)$. The fraction of active sediments has been taken as $f = 0.5$ for the whole estuary (Periáñez et al., 2005). Although this parameter will probably change from one position to another, the

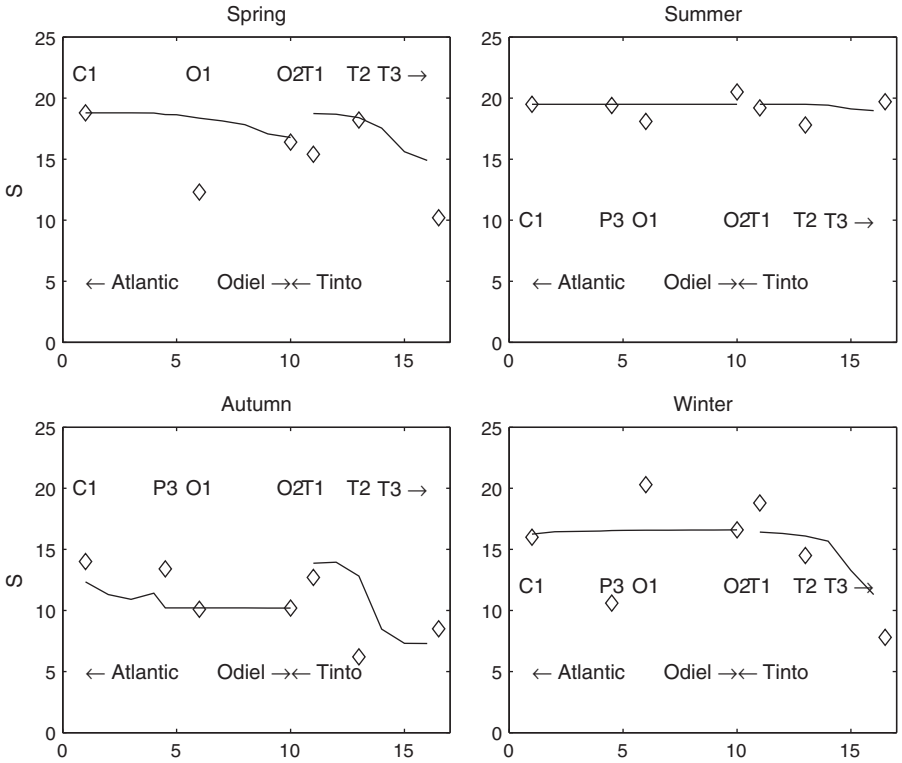

Fig. 4. Comparison between measured (points) and calculated (lines) chlorinity values (ppt) along the estuary for each sampling campaign. The Odiel River extends in the *x* axis from 1 to 10 and the Tinto River from 10 (confluence with Odiel) to 15. The name of each sample is indicated, and point positions may be seen in the map in Fig. 1.

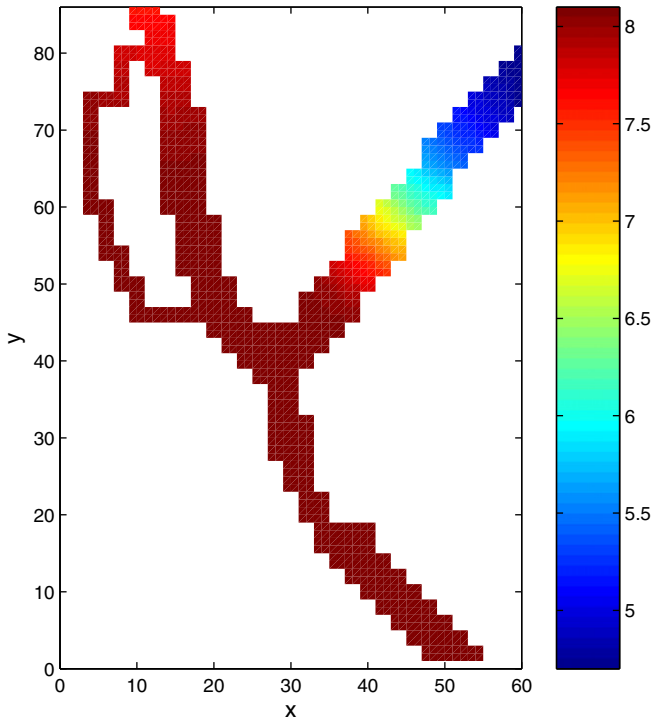

Fig. 5. Computed pH distribution over the estuary in spring. Each number in the *x* and *y* axis gives the grid cell number (thus each unit corresponds to 125 m).

selection of a constant (but realistic) value seems enough to describe the general dispersion patterns of the different radionuclides. Following previous work (Periáñez et al., 2005), $L=0.01$ m and $\phi=0.1$ are used.

Note that in these models the bed sediment is treated in the same way as suspended matter (if it were included). The amount of sediment particles which may adsorb radionuclides from the water column depends on the sediment bulk density, the fraction of fine particles in the bed and on the sediment mixing depth. The mass of sediment per unit surface area of the estuary is $\rho_s f L$. The equivalent particle concentration in the water column, resulting from this mass, is $\rho_s f L/H$. Using the orders of magnitude from Table 1 and $H\sim 1$ m, this leads to a bed sediment concentration of de order of 1 kg/m^3. This is two orders of magnitude higher than typical suspended matter concentration in the estuary, of the order of 10^{-2} kg/m^3 (Bolívar et al., 2000; Periáñez et al., 1996). Thus the amount of bed sediment available for adsorption is two orders of magnitude higher than the amount of suspended matter particles, which have been neglected. Of course, in the case of a 3D model this reasoning would not be strictly valid.

Radionuclides enter the estuary through contaminated river water inflow (defined in open boundary conditions, see Section 2.5), but also as a result of leaching from the phosphogypsum piles located by the Tinto River. This leaching occurs during rain periods. Thus, radionuclide input from the piles, I, has been directly correlated with daily precipitation, R, in the form $I=\Pi R$, where Π is calibrated for each radionuclide through a trial and error process. Calibration is required because, although radionuclide concentration in leached water is known (see Section 1), the volume of leached water during each rain episode is not known. The factor Π has resulted 30 times higher for ^{238}U than for ^{226}Ra.

The method to obtain the different kinetic rates is described in what follows. The exchange velocity may be deduced from the expression relating the non-dimensional distribution coefficient, k_d', with kinetic rates for a two-reaction model:

$$k_d' = \frac{k_1}{k_2}\left(1+\frac{k_3}{k_4}\right) \tag{18}$$

Table 1
Summary of model parameters.

Parameter description	Value	Source
Diffusion coefficient	$K_D=0.61$ m^2/s	Breton and Salomon (1995)
50% saturation chlorinity	$S_0=15.8$ ppt	Laissaoui et al. (1998)
χ_1 dependence with pH	$\alpha=5$	fit to data in USEPA (1999)
χ_1 dependence with pH	$\beta=5$	fit to data in USEPA (1999)
Particle density	$\rho=2600$ kg/m^3	standard value
Sediment bulk density	$\rho_s=900$ kg/m^3	measured
Mixing depth	$L=0.01$ m	Periáñez et al. (2005)
Correction factor	$\phi=0.1$	Periáñez et al. (2005); Periáñez (2009)
Fine sediment fraction	$f=0.5$	Periáñez et al. (2005)
Kinetic rate	$k_2=8.17\times10^{-6}$ s^{-1}	Laissaoui et al. (1998)
Kinetic rate	$k_3=1.40\times10^{-7}$ s^{-1}	El Mrabet et al. (2001)
Kinetic rate	$k_4=1.40\times10^{-8}$ s^{-1}	Barros et al. (2004), Ciffroy et al. (2001)
^{226}Ra freshwater k_d	$k_d^0=7.4$ m^3/kg	IAEA (2010)
^{238}U freshwater k_d	$k_d^0=1.7\times10^{-2}$ m^3/kg	USEPA (1999)

Using Eqs. (7) and (8), and converting the non-dimensional k_d' to a dimensional one (k_d, measured in m^3/kg), it is obtained that

$$k_d = \frac{\chi_1}{k_2}\left(1+\frac{k_3}{k_4}\right)\frac{3\phi}{\rho r} \tag{19}$$

If the k_d and kinetic rates k_2, k_3 and k_4 are known, χ_1 may be calculated from this equation.

The coefficient k_2 was obtained from adsorption laboratory experiments carried out with ^{133}Ba, a γ emitter whose chemical behavior is very similar to that of Ra. They were carried out with unfiltered water of the Odiel estuary in such a way that laboratory conditions (temperature, pH, salinity, movement of water) were as close as possible to the natural conditions. The time increase of ^{133}Ba activity in suspended sediments enables the coefficient to be calculated (Laissaoui et al., 1998). The value obtained was $k_2=8.17\times10^{-6}$ s^{-1}.

Barros et al. (2004) have carried out sorption experiments with ^{133}Ba. They have obtained that the relation $k_4\simeq k_3/10$ holds between rates governing the second consecutive reaction. Nevertheless, kinetic rates obtained by Barros et al (2004) cannot be directly used in this model since they prepared artificial sediment suspensions with given particle sizes. Ciffroy et al. (2001) have found a similar relation for some radionuclides. Thus, we have used in the model that $k_4=k_3/10$.

On the other hand, El Mrabet et al. (2001) have measured a value of 1.4×10^{-7} s^{-1} for k_3 in their experiments carried out with sea water from the southwest coast of Spain. These experiments were carried out with Pu and are probably not totally adequate for describing the behavior of other radionuclides. However, this value has been used due to the lack of data concerning ^{226}Ra and ^{238}U. In summary, we have used the following values since acceptable results are obtained with them: $k_3=1.4\times10^{-7}$ s^{-1} and $k_4=1.4\times10^{-8}$ s^{-1}. Ideally, site-specific kinetic rates should be used. Nevertheless, sensitivity tests have been carried out to study the model response to changes in kinetic rates governing the second reaction. They were described in Periáñez et al. (2005) and are not repeated here.

As described before (Nyffeler et al., 1984), k_2 is very similar even for elements with a rather different geochemical behaviour, being χ_1 the essential parameter describing the tracer geochemical behavior. Thus, the same value is given to k_2, k_3 and k_4 for isotopes of Ra, U and Th. This approach has been successfully used in earlier simulations in the Odiel–Tinto estuary (Periáñez et al., 2005), in the Strait of Gibraltar–Alborán Sea (Periáñez, 2008) for several elements (Ra, Cs, and Pu) and in the Gulf of Cadiz for heavy metal dispersion (Periáñez, 2009).

In summary, the freshwater distribution coefficient k_d^0 has been defined for each radionuclide. Using Eq. (19) and rates k_2, k_3 and k_4 defined above, the freshwater exchange velocity χ_1^0 is calculated for

each radionuclide. Finally, the actual exchange velocity χ_1 for each location and time is calculated, using Eq. (12), for the local pH and chlorinity values. A summary of model parameters, together with their sources, is given in Table 1.

3.2.2. Model results

A comparison between calculated and measured (Hierro, 2009; Hierro et al., 2012) ^{226}Ra sediment concentrations is presented in Fig. 6 for the four seasonal sampling campaigns. Concentration levels along the estuary are in general correctly reproduced by the model for the different campaigns. These concentrations are of the order of 40 Bq/kg, decreasing as going along the Odiel–Tinto common channel towards the Atlantic Ocean. A high ^{226}Ra concentration has been measured for several campaigns in sample T1, in the Odiel–Tinto confluence. This enhanced value is not reproduced by the model.

Results for ^{238}U are given in Fig. 7. The general trends along the estuary are well reproduced by the model. It may be seen that concentration levels are significantly higher in the Tinto than in the Odiel River. Concentrations in the Tinto River generally decrease as going downstream towards the confluence with the Odiel River. Also, ^{238}U concentrations are significantly higher than ^{226}Ra concentrations.

As an additional result, the computed distribution of ^{226}Ra over the estuary for September 2009 is presented in Fig. 8 as an example. It may be seen that the Tinto River is slightly more contaminated than the Odiel, due to radionuclide input from the phosphogypsum piles. Concentration levels decrease along the channel connecting with the Atlantic Ocean.

Some numerical experiments have been carried out to evaluate the relative significance of the different radionuclide sources (input from rivers and phosphogypsum piles) and, also, to evaluate the influence of estuarine circulation on the distribution and levels of radionuclides.

A first experiment consisted of simulating ^{226}Ra behavior if inputs from rivers or from phosphogypsum piles are not included. Results are summarized in Fig. 9. Two conclusions are clearly deduced. First, that the main radionuclide source into the Odiel River is due to contaminated water entering the estuary from the upstream river. Effectively, there are not any differences in results for the Odiel River if input from phosphogypsum piles is or is not included. However, concentration levels in sediments are much lower than measured levels if the input of radionuclide through the northern open boundary is set to zero. Also, it is interesting to notice that some contamination reaches the upper part of the Odiel River (the region from samples O1 to O2) although water entering through the northern open boundary is clean. This is due to the mixing induced by tides. The second conclusion is that both sources (river supplies and leaching from phosphogypsum piles) contribute in a similar way to concentration levels in the Tinto River.

The same experiment, but in the case of ^{238}U, is presented in Fig. 10. Results with and without input from phosphogypsum piles cannot be distinguished. It is clear that measured ^{238}U levels in the estuary are almost entirely due to the inflow of contaminated water from upstream. The significance of the phosphogypsum piles as a radionuclide source to the Tinto River is higher for ^{226}Ra than for ^{238}U, in spite of the fact that water leached from the piles contains a ^{238}U concentration which is, on average, 30 times higher than that of ^{226}Ra (see Sections 1 and 3.2.1). This release of ^{238}U from the phosphogypsum piles is almost entirely masked by the high uranium amounts entering the estuary from the upstream river.

Numerical experiments indicate that rivers constitute a very significant source of radionuclides to the estuary, in spite of their generally very low stream flows. From the estuary, radionuclides and metals are introduced into the Atlantic Ocean. Indeed, it has already been found (Elbaz-Poulichet et al., 2001; Periáñez, 2009) that coastal waters transport dissolved metals from the Odiel–Tinto rivers to a distance of more than 200 km along the southwest coast of Spain.

The effects of water circulation on radionuclide sediment concentration levels are analyzed in Fig. 11 using ^{226}Ra as an example (the same conclusions are obtained if uranium is used in the numerical experiments). If tides are not included in calculations, but only currents produced by river flows, radionuclide concentrations are significantly higher than measured values. This highlights the relevance of tides in

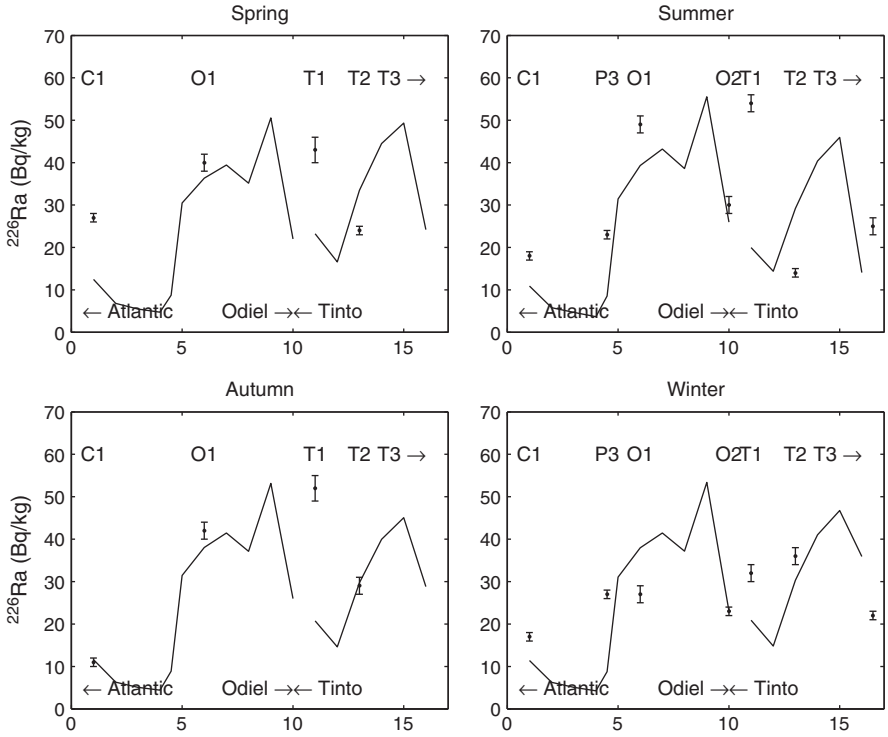

Fig. 6. Comparison between measured (points) and calculated (lines) ^{226}Ra sediment concentrations values (Bq/kg) along the estuary for each sampling campaign. The Odiel River extends in the *x* axis from 1 to 10 and the Tinto River from 10 (confluence with Odiel) to 15. The name of each sample is indicated, and point positions may be seen in the map in Fig. 1.

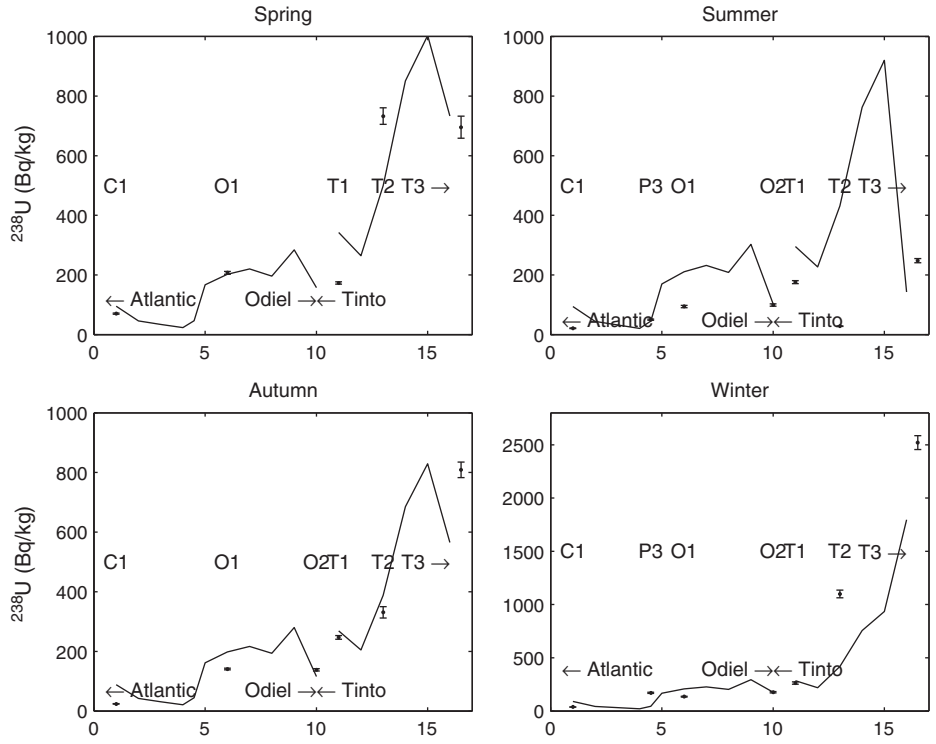

Fig. 7. Same as Fig. 6 but for ^{238}U.

mixing processes and reducing contamination levels in the estuary. Note that not including tides means that seawater does not enter the estuary, but only water discharged by the rivers leaves the estuary because of mass conservation. Concentrations are more enhanced along the Tinto than along the Odiel River if tides are not included in the calculation. Sediments may act as a delayed radionuclide source to the water column or as a radionuclide sink, depending on the radionuclide concentration in the sediment and in the dissolved phase. Tinto River flow is lower than that of the Odiel, thus sediments are more slowly washed by water (if acting as a delayed source) and, if they act as a sink, absorb more radionuclides due to the slower current and consequently larger water-sediment contact time. The result in any case is a higher contamination of Tinto River sediments with respect to the Odiel River if tidal currents are not considered in the calculations.

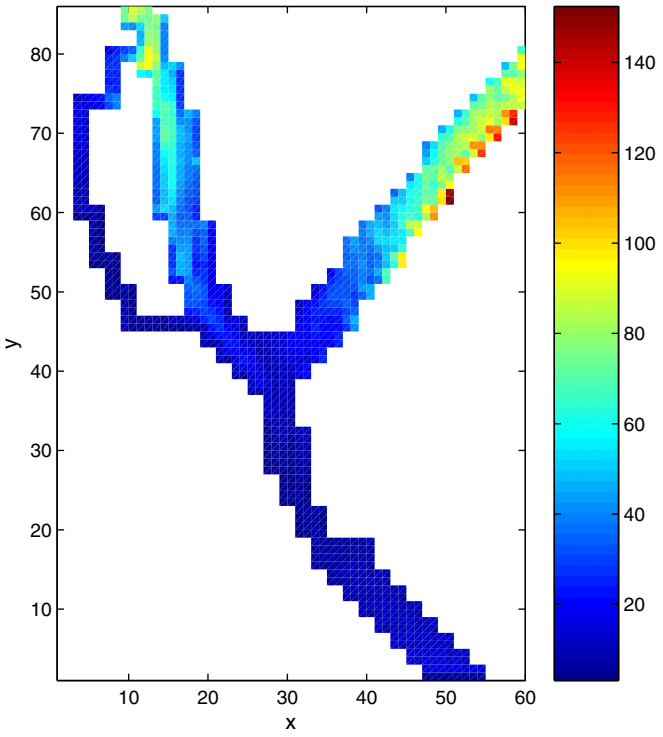

Fig. 8. Computed distribution of ^{226}Ra in sediments (Bq/kg), for September 2009, over the estuary. Each number in the *x* and *y* axis gives the grid cell number (thus each unit corresponds to 125 m).

On the other hand, if tides are included but currents due to river flows are not, results are essentially the same as for the nominal simulation (with both tidal and river flow induced currents). This should not be an unexpected result due to the generally very low river flows: average values for the Odiel and Tinto rivers of 14.8 and 2.9 m^3/s respectively (López-González et al., 2005; Sarmiento et al., 2005). Indeed, if an experiment in which river flows are increased by a factor 10 (blue line in Fig. 11), results are not very different to the nominal simulation. Only downstream transport of radionuclides is slightly increased. This is again confirming the essential role played by tides in controlling transport and mixing in the estuary, due to the low (even if artificially increased by one order of magnitude) river flows.

The sensitivity of the model formulation to variations in the different parameters has already been studied in great detail and is not repeated here (Periáñez, 2004b). In particular, sensitivity of formulation (in the specific model application to the Odiel–Tinto estuary) to mixing depth and correction factor ϕ is studied in Periáñez (2002) and to kinetic rates governing the second reaction (k_3 and k_4) in Periáñez et al. (2005).

4. Conclusions

A numerical model of the Odiel–Tinto estuary, affected by AMD and industrial activities, has been developed. Water currents produced by tides and river stream flows have been calculated. Currents are then used to obtain seasonal pH and chlorinity distributions, since variations

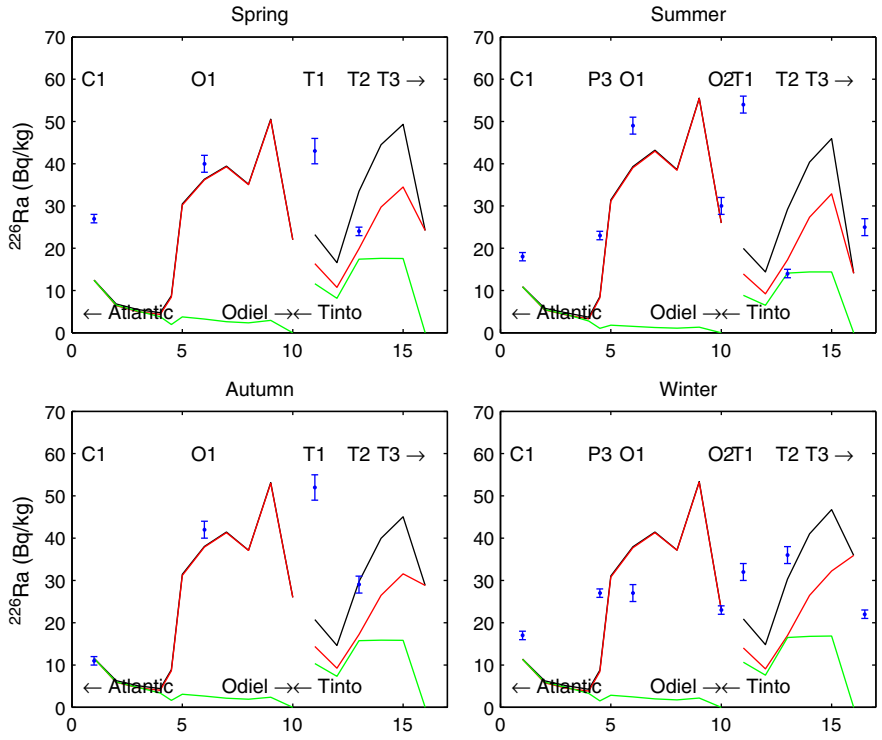

Fig. 9. Comparison between measured (points) and calculated (lines) ^{226}Ra sediment concentrations values (Bq/kg) along the estuary for each sampling campaign. The black line corresponds to the nominal simulation (Fig. 6), the red line is the result without input from phosphogypsum piles and the green line is result without radionuclide supplies from rivers.

in environmental conditions affect the distribution of radionuclides between water and sediments. These processes are described in a dynamic way, using kinetic transfer coefficients. A formulation has been developed to describe the dependence of kinetic coefficients with pH and chlorinity. Calculated currents, pH and chlorinity distributions are then used to simulate radionuclide dispersion.

The model has been applied to ^{226}Ra and ^{238}U. Calculated concentrations of these radionuclides in sediments have been compared

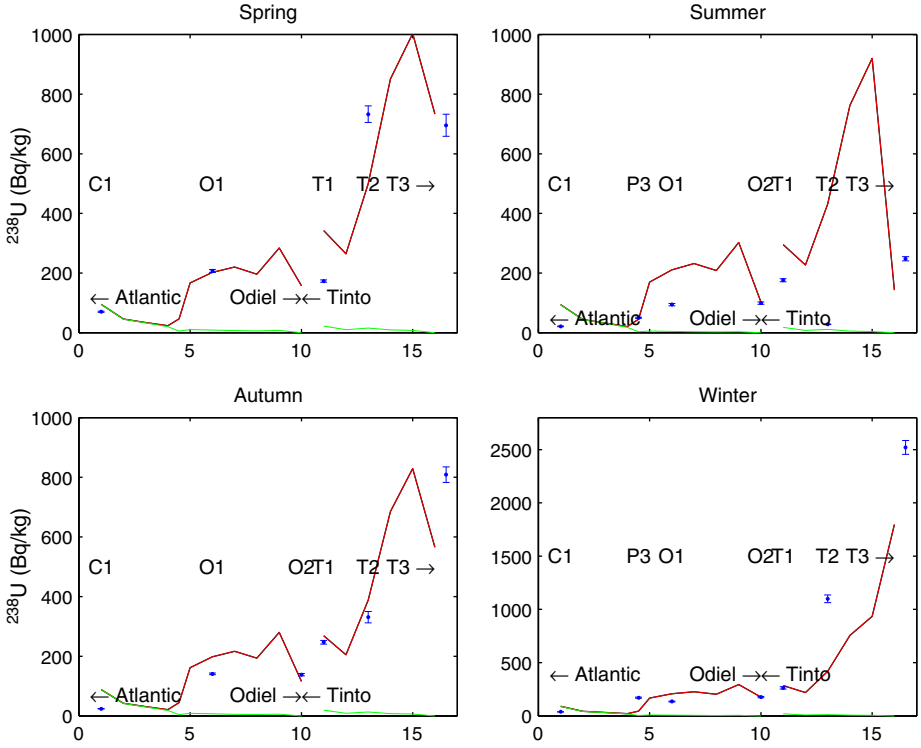

Fig. 10. Comparison between measured (points) and calculated (lines) ^{238}U sediment concentrations values (Bq/kg) along the estuary for each sampling campaign. The black line corresponds to the nominal simulation (Fig. 7), the red line is the result without input from phosphogypsum piles and the green line is result without radionuclide supplies from rivers. Red and black lines cannot be distinguished.

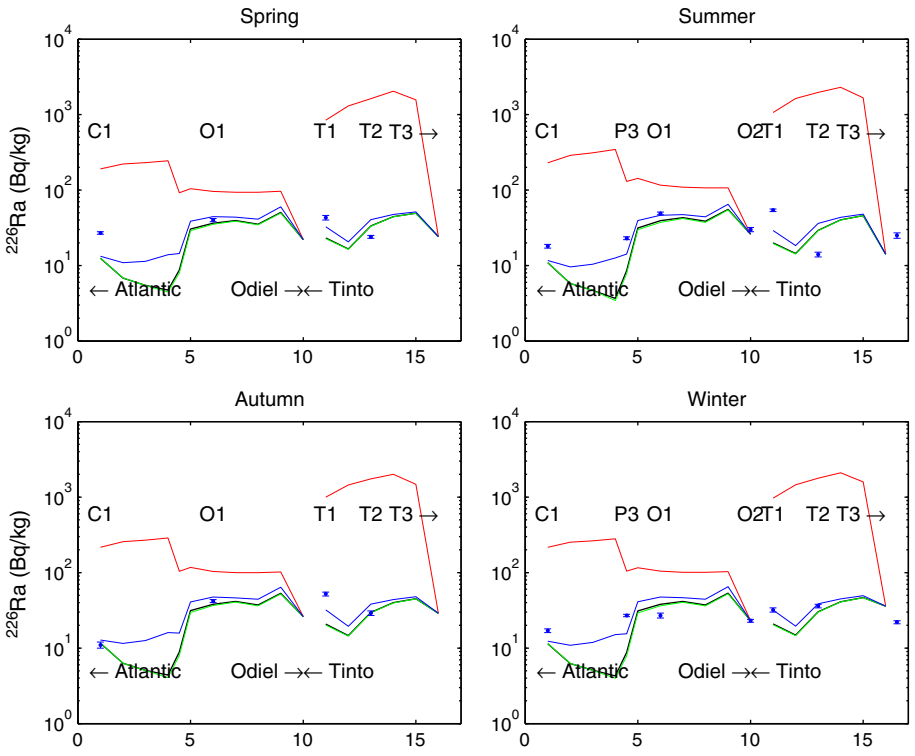

Fig. 11. Comparison between measured (points) and calculated (lines) ^{226}Ra sediment concentrations values (Bq/kg) along the estuary for each sampling campaign. The black line corresponds to the nominal simulation (Fig. 6), the red line is the result without tides, the green line is result without currents due to river flows and the blue line is results with river flows increased by a factor 10. Green and black lines cannot be distinguished. Logarithmic scale has been used to appreciate details.

with measurements obtained from four seasonal sampling campaigns. In general, distribution patterns and concentration levels are reasonably well reproduced by the model. This means that processes have been adequately described. It is relevant to notice that the dispersion of radionuclides with very different geochemical behaviors could be simulated with the present model formulation.

Some numerical experiments have also been carried out. The main conclusions are the following:

- Tides are essential in keeping relatively low concentration levels in the estuary, due to the mixing induced by them.
- In spite of the low stream flows of the rivers, they constitute a very significant source of radionuclides into the estuary.
- Leaching of radionuclides from the phosphogypsum piles into the Tinto River is not significant for ^{238}U, although in the case of ^{226}Ra contributes to some 50% of contamination levels of the river.

Acknowledgments

Work is supported through the projects “Determination of scavenging rates and sedimentation velocities using reactive-particle radionuclides in coastal waters; application to pollutants dispersion modeling”, Ref. CTM2009-14321-C02-01, funded by the Spanish Ministerio de Ciencia e Innovación and “Characterization and modeling of the phosphogypsum stacks from Huelva for their environmental management and control” (Ref. RNM-6300), funded by the Government of Andalusia.

References

Abril, J.M., Fraga, E., 1996. Some physical and chemical features of the variability of k_d distribution coefficients for radionuclides. J. Environ. Radioact. 30, 253–270.
Absi, A., Villa, M., Moreno, H.P., Manjón, G., Periáñez, R., 2004. Self-cleaning in an estuarine area formerly affected by ^{226}Ra anthropogenic discharges. Sci. Total. Environ. 329, 183–195.
Aston, S.R., Assinder, D.J., Kelly, M., 1985. Plutonium in intertidal and estuarine sediments in the northern Irish Sea. Estuarine Coastal Shelf Sci. 20, 761–771.
Barros, H., Laissaoui, A., Abril, J.M., 2004. Trends of radionuclide sorption by estuarine sediments. Experimental studies using ^{133}Ba as a tracer. Sci. Total. Environ. 319, 253–267.
Bolívar, J.P., García-Tenorio, R., Vaca, F., 2000. Radioecological study of an estuarine system located in the south of Spain. Water Res. 34, 2941–2950.
Bolívar, J.P., García-Tenorio, R., Mas, J.L., Vaca, F., 2002. Radioactive impact in sediments from an estuarine system affected by industrial waste releases. Environ. Int. 27, 639–645.
Bolívar, J.P., Martín, J.E., García-Tenorio, R., Pérez-Moreno, J.P., Mas, J.L., 2009. Behaviour and fluxes of natural radionuclides in the production process o a phosphoric acid plant. Appl. Radiat. Isot. 67, 345–356.
Breton, M., Salomon, J.C., 1995. A 2D long term advection dispersion model for the Channel and southern North Sea. J. Mar. Syst. 6, 495–513.
Ciffroy, P., Garnier, J.M., Pham, M.K., 2001. Kinetics of the adsorption and desorption of radionuclides of Co, Mn, Cs, Fe, Ag and Cd in freshwater systems: experimental and modelling approaches. J. Environ. Radioact. 55, 71–91.
de la Torre, M.L., Grande, J.A., Graiño, J., Gómez, T., Cerón, J.C., 2011. Characterization of AMD pollution in the River Tinto (SW Spain). Geochemical comparison between generating source and receiving environment. Water Air Soil Pollut. 216, 3–19.
Duursma, E.K., Carroll, J., 1996. Environmental Compartments. Springer, Berlin.
Dyke, P.P.G., 2001. Coastal and Shelf Sea Modelling. Kluwer, The Netherlands.
El Mrabet, R., Abril, J.M., Manjón, G., García-Tenorio, R., 2001. Experimental and modelling study of plutonium uptake by suspended matter in aquatic environments from southern Spain. Water Res. 35, 4184–4190.
Elbaz-Poulichet, F., Morley, N.H., Beckers, J.M., Nomerange, P., 2001. Metal fluxes through the Strait of Gibraltar: the influence of the Odiel and Tinto rivers (SW Spain). Mar. Chem. 73, 193–213.
Elliott, A.J., Clarke, S., 1998. Shallow water tides in the Firth of Forth. Hydrogr. J. 87, 19–24.
Hierro, A., 2009. Radionucleidos naturales en sedimentos recientes de la Ría de Huelva. Tesina Fin de Máster. Dept. of Applied Physics, University of Huelva (in Spanish).
Hierro, A., Bolívar, J.P., Vaca, F., Baskaran, M., 2012. Behaviour of natural radionuclides in current sediments from an estuary affected by acid mine drainage and industrial discharges. J. Environ. Radioact. 110, 13–23.
IAEA, 2010. Handbook of parameter values for the prediction of radionuclide transfer in terrestrial and freshwater environments. TRS-472 International Atomic Energy Agency, Vienna.
Ibañez, C., Caiola, N., Nebra, A., Wessels, M., 2009. Estuarios. Bases ecológicas preliminares para la conservación de los tipos de hábitat de interés comunitario en España. Ministerio de Medio Ambiente, y Medio Rural y Marino, Madrid. 75 pp. (in Spanish).
Kowalick, Z., Murty, T.S., 1993. Numerical Modelling of Ocean Dynamics. World Scientific, Singapore.

Laissaoui, A., Abril, J.M., Periáñez, R., García-León, M., García-Montaño, E., 1998. Kinetic transfer coefficients for radionuclides in estuarine waters: reference values for ^{133}Ba and effects of salinity and suspended load concentration. J. Radioanal. Nucl. Chem. 237, 55–61.

Lam, D.C.L., Murthy, C.R., Simpson, R.B., 1984. Effluent Transport and Diffusion Models for the Coastal Zone. Lecture Notes on Coastal and Estuarine Studies. Springer, Berlin.

López-González, N., Borrego, J., de la Rosa, J., Grande, J.A., Carro, B., Lozano-Soria, O., 2005. Rare earth concentration and fractionation in the water of the fluvio-marine system of the Tinto River (SW Spain). Geogaceta 38, 151–154.

Martín, J.E., García-Tenorio, R., San Miguel, E.G., Respaldiza, M.A., Bolívar, J.P., Alves, L.C., da Silva, M.F., 2002. Historical impact in an estuary of some mining and industrial activities evaluated through the analysis by TTPIXE of a dated sediment core. Nucl. Instrum. Methods Phys. Res. B 189, 153–157.

Martínez-Aguirre, A., García-León, M., Gascó, C., Travesi, A., 1996. Anthropogenic emissions of ^{210}Po, ^{210}Pb, and ^{226}Ra in an estuarine environment. J. Radioanal. Nucl. Chem. 207, 357–367.

Nyffeler, U.P., Li, Y.H., Santschi, P.H., 1984. A kinetic approach to describe trace element distribution between particles and solution in natural aquatic systems. Geochim. Cosmochim. Acta 48, 1513–1522.

Periáñez, R., 1999. Three dimensional modelling of the tidal dispersion of non conservative radionuclides in the marine environment: application to ^{239,240}Pu dispersion in the eastern Irish Sea. J. Mar. Syst. 22, 37–51.

Periáñez, R., 2002. The enhancement of ^{226}Ra in a tidal estuary due to the operation of fertilizer factories and redissolution from sediments: experimental results and a modelling study. Estuarine Coastal Shelf Sci. 54, 809–819.

Periáñez, R., 2003. Kinetic modelling of the dispersion of plutonium in the eastern Irish Sea: two approaches. J. Mar. Syst. 38, 259–275.

Periáñez, R., 2004a. Testing the behaviour of different kinetic models for uptake-release of radionuclides between water and sediments when implemented on a marine dispersion model. J. Environ. Radioact. 71, 243–259.

Periáñez, R., 2004b. On the sensitivity of a marine dispersion model to parameters describing the transfers of radionuclides between the liquid and solid phases. J. Environ. Radioact. 73, 101–115.

Periáñez, R., 2005. Modelling the Dispersion of Radionuclides in the Marine Environment. Springer-Verlag, Heidelberg.

Periáñez, R., 2008. A modelling study on ^{137}Cs and ^{239,240}Pu behaviour in the Alborán Sea, western Mediterranean. J. Environ. Radioact. 99, 694–715.

Periáñez, R., 2009. Environmental modelling in the Gulf of Cadiz: heavy metal distributions in water and sediments. Sci. Total. Environ. 407, 3392–3406.

Periáñez, R., Abril, J.M., García-León, M., 1996. Modelling the suspended matter distribution in an estuarine system. Application to the Odiel River in southwest Spain. Ecol. Model. 87, 169–179.

Periáñez, R., Absi, A., Villa, M., Manjón, G., Moreno, H.P., 2005. Self-cleaning in an estuarine area formerly affected by ^{226}Ra anthropogenic enhancements: numerical simulations. Sci. Total. Environ. 339, 207–218.

Proctor, R., Flather, R.A., Elliott, A.J., 1994. Modelling tides and surface drift in the Arabian Gulf: application to the Gulf oil spill. Cont. Shelf Res. 14, 531–545.

Pugh, D.T., 1987. Tides, Surges and Mean Sea Level. Wiley, Chichester.

Rajkovic, M.B., Karljikovic-Rajic, K., Vladjisavlevic, G.T., Ciric, I.S., 1999. Investigation of radionuclides in phosphogypsum. Meas. Tech. 42, 64–68.

Respaldiza, M.A., López-Tárrida, A.J., Gómez-Camacho, J., 1993. Environmental control of Tinto and Odiel river basins by PIXE. Nucl. Instrum. Methods Phys. Res. B 75, 334–337.

Ruiz, F., 2001. Trace metals in estuarine sediments of south-western Spain. Mar. Pollut. Bull. 42, 481–489.

Sainz, A., Ruiz, F., 2006. Influence of the very polluted inputs of the Tinto–Odiel system on the adjacent littoral sediments of southwestern Spain: a statistical approach. Chemosphere 62, 1612–1622.

Sarmiento, A.M., Casiot, C., Nieto, J.M., Elbaz-Poulichet, F., Olías, M., 2005. Seasonal variations in Fe and As speciation and mobility in waters affected by acid mine drainage in the Odiel River basin (Huelva, Spain). Geogaceta 37, 115–118.

USEPA, 1999. Understanding Variation in Partition Coefficient, k_d, Values, volume 2. EPA 402-R-99-004B.

Van der Heijde, H.B., Klijn, P.J., Passchier, W.F., 1988. Radiological impact of the disposal of phosphogypsum. Radiat. Prot. Dosim. 24, 419–423.

Vested, H.J., Baretta, J.W., Ekebjærg, L.C., Labrosse, A., 1996. Coupling of hydrodynamical transport and ecological models for 2D horizontal flow. J. Mar. Syst. 8, 255–267.